Journal of Experimental Botany, Vol. 62, No. 3, pp. 1001–1015, 2011
doi:10.1093/jxb/erq332 Advance Access publication 9 November, 2010

Journal of Experimental Botany
www.jxb.oxfordjournals.org

RESEARCH PAPER

Brachypodium distachyon grain: characterization of endosperm cell walls

Fabienne Guillon[1,*], Brigitte Bouchet[1], Frédéric Jamme[2], Paul Robert[1], Bernard Quéméner[1], Cécile Barron[3], Colette Larré[1], Paul Dumas[4] and Luc Saulnier[1]

[1] INRA UR1268 Biopolymers, Interactions Assemblies, F-44316 Nantes, France
[2] INRA Department CEPIA, F-44316 Nantes, France
[3] INRA, UMR 1208 'Agropolymers Engineering and Emerging Technologies', INRA-CIRAD-UMII-Supagro, F-34000 Montpellier, France
[4] Synchrotron SOLEIL, L'orme des Merisiers, BP 48, Saint Aubin, F-91192 Gif sur Yvette, France

* To whom correspondence should be addressed. E-mail: abienne.guillon@nantes.inra.fr

Received 13 July 2010; Revised 24 September 2010; Accepted 24 September 2010

Abstract

The wild grass *Brachypodium distachyon* has been proposed as an alternative model species for temperate cereals. The present paper reports on the characterization of *B. distachyon* grain, placing emphasis on endosperm cell walls. *Brachypodium distachyon* is notable for its high cell wall polysaccharide content that accounts for ~52% (w/w) of the endosperm in comparison with 2–7% (w/w) in other cereals. Starch, the typical storage polysaccharide, is low [<10% (w/w)] in the endosperm where the main polysaccharide is (1–3) (1–4)-β-glucan [40% (w/w) of the endosperm], which in all likelihood plays a role as a storage compound. In addition to (1–3) (1–4)-β-glucan, endosperm cells contain cellulose and xylan in significant amounts. Interestingly, the ratio of ferulic acid to arabinoxylan is higher in *B. distachyon* grain than in other investigated cereals. Feruloylated arabinoxylan is mainly found in the middle lamella and cell junction zones of the storage endosperm, suggesting a potential role in cell–cell adhesion. The present results indicate that *B. distachyon* grains contain all the cell wall polysaccharides encountered in other cereal grains. Thus, due to its fully sequenced genome, its short life cycle, and the genetic tools available for mutagenesis/transformation, *B. distachyon* is a good model to investigate cell wall polysaccharide synthesis and function in cereal grains.

Key words: Arabinoxylan, (1–3) (1–4)-β-glucan, cereal, enzymatic fingerprinting, FT-IR microspectrocopy, immunolabelling.

Introduction

Cereal grains are the most important renewable resource for food, fodder, and industrial raw material. The main cereal crops are wheat, rice, rye, maize, barley, oats, sorghum, and millets. Botanically, cereal grains classified as caryopses share many common attributes. In all species, the endosperm makes the greatest contribution to the whole dry weight and determines the value of the crops in both quantitative and qualitative terms. The major components are starch (60–70% of grain, 70–80% of flour) and proteins (10–15%) which serve as a reservoir of carbon, nitrogen, and sulphur for post-germination seedlings. Cell walls only account for ~3–8% of the total grain weight. In grain, they fulfil a variety of physiological functions. They provide the skeletal framework for the tissues and the intercellular cohesiveness that maintains tissue integrity. Very recently, a report indicated that the expression of heterologous enzymes involved in arabinoxylan (AX) degradation (endoxylanase and ferulic acid esterase) produces shrivelled grains drastically altered in average weight (Harholt *et al.*, 2010). During grain development and germination, the cell

Abbreviations: AX, arabinoxylan; BSA, bovine serum albumin; BG_3, 3-*O*-β-cellobiosyl-D-glucose; BG_4, 3-*O*-β-cellotriosyl-D-glucose; CBM3a, crystalline cellulose-binding module 3a; 5-O-Fer-Ara, 5-*O*-(trans-feruloyl)-L-arabinose; FT-IR, Fourier transform infrared; GOS, gluco-oligosaccharides; HPAEC, high-performance anion exchange chromatography; PBS, 0.1 M Na-phosphate buffer saline; UX, unknown arabino-xylo-oligosaccharides.

walls can be a source of easily mobilized reserve material (Buckeridge *et al.*, 2004). Although present in minor amounts in the endosperm, they have major effects on the use of cereal grains (milling, baking, and animal feed uses). As a dietary fibre, they have a major impact on the nutritional quality of cereal foods (Izydorczyk and Biliaderis, 2007; Saulnier *et al.*, 2007*a*; Izydorczyk and Dexter, 2008). The composition of cell walls in cereals differs from that of most other land plants. In cereals, the endosperm cell walls mainly consist of AX carrying ester-linked ferulic acid residues and (1–3) (1–4)-β-glucan, with only low levels of cellulose, glucomannan, and structural proteins (Fincher and Stone, 1986). Pectic polysaccharides and xyloglucan have been reported in rice endosperm cell walls (Shibuya and Iwasaki, 1978; Shibuya and Nakane, 1984), but not in other cereals. The relative proportions of (1–3) (1–4)-β-glucan and AX vary significantly according to the type of cereal: rye, wheat, and sorghum are rich in AX, whereas barley and oat exhibit high levels of (1–3) (1–4)-β-glucan (Fincher and Stone, 1986; Lazaridou *et al.*, 2007; Saulnier *et al.*, 2007*b*).

Genetic and genetic engineering strategies have been employed to increase the nutritional value and processing performance of cereal grains. However, further improvement requires a better understanding of the biochemical mechanism underlying endosperm development. The use of *Arabidopsis thaliana* and rice (*Oryza sativa*) as model plants has greatly accelerated research in plant biology. However, these plant models present drawbacks to addressing biological questions related to temperate grasses. The dicot *A. thaliana* and, to a lesser extent, the monocot rice are both phylogenetically far from temperate grasses such as wheat. In addition, rice is not very attractive as a model due to its long life cycle. Consequently, the emergence of *Brachypodium distachyon* as a plant model offers an alternative. *Brachypodium distachyon* belongs to the Brachypodieae tribe, which is sister of Triticeae, Poeae, Bromeae, and Avenae (Kellogg, 2001; Vogel *et al.*, 2006; Opanowicz *et al.*, 2008; Bolot *et al.*, 2009). It possesses a small genome whose sequence and comparative genomics are available and published (International Brachypodium Initiative, 2010, http://www.brachypodium.org/node/8). *Brachypodium distachyon* has a relatively low repetitive DNA content (Catalan *et al.*, 1995), and tools [microarrays, an expressed sequence tag (EST) collection, and a bacterial artificial chromosome (BAC) library] for molecular genetic analyses are being developed (Hasterok *et al.*, 2004; Vogel *et al.*, 2006; Doust, 2007; Garvin *et al.*, 2008; Huo *et al.*, 2008; Opanowicz *et al.*, 2008). *Brachypodium distachyon* can be genetically transformed using *Agrobacterium* with relative ease (Vain *et al.*, 2008; Vogel and Hill, 2008). In addition, its small stature, short life cycle (~4 months), and simple growth conditions make it amenable to high-throughput mutant screens (Draper *et al.*, 2001).

With a large seed relative to the plant size, *B. distachyon* is suitable for studies on seed development and grain filling. Unlike the rice caryopsis, the *B. distachyon* grain has a crease (Laudencia-Chingcuaco and Vensel, 2008), a feature found to be interesting from a developmental point of view.

To date, information on *B. distachyon* grain composition is scarce. Laudencia-Chingcuanco and Vensel (2008) showed that the main storage proteins are 12S and 7S globulins. A characterization of the 12S globulins revealed that they are salt insoluble and therefore belong to the glutelins (Larré *et al.*, 2010). These results strengthen the idea that *B. distachyon* is closer to oat and rice than to *Triticum*, although phylogenetic analysis indicates that *B. distachyon* is ancestral and equally related to *Avena* and *Triticum* (Kellogg, 2001).

The present work aimed to gain insight into the usefulness of *B. distachyon* as a model for cell wall studies of cereal grains. An overall characterization of *B. distachyon* grain with a special focus on the endosperm was undertaken. Basic information on the grain morphology and global composition (starch, proteins, and cell wall polymers) is provided, together with detailed information on cell wall composition and structure obtained using several complementary techniques.

Materials and methods

Materials

Seed samples of *B. distachyon* were a gift from Dr M. Gonnaud (TGU Institut Jean-Pierre Bourgin, INRA Versailles, France).

Endoxylanase (EC 3.2.1.8, xylanase M1) from *Trichoderma viride* and lichenase [endo-1,3(4)-β-D-glucanase, EC 3.2.1.73] from *Bacillus subtilis* were purchased from Megazyme (www.megazyme.com). The xylanase activity determined by the supplier for water-extractable AX (40 °C, pH 4.5) was 1670 U ml^{-1}. The pH optimum range was 4.5–5.0. The lichenase activity determined by the supplier for barley (1–3) (1–4)-β-glucan (40 °C, pH 6.5) was 1000 U ml^{-1}. The pH optimum range was 6.5–7.0.

All chemicals were of pure grade and purchased from Amersham Pharmacia Biotech (http://www.apbiotech.com) and Sigma Chemicals (http://www.sigmaaldrich.com).

The reference polysaccharides were AX prepared in the laboratory as previously described (Dervilly *et al.*, 2000), and cellulose and (1–3) (1–4)-β-glucan purchased from Sigma-Aldrich (http://www.sigmaaldrich.com) and Megazyme (www.megazyme.com), respectively.

Affinity probes

The affinity probes used were mouse monoclonal antibody against AX (anti-AX1), mouse monoclonal antibody against (1–3) (1–4)-β-glucan [anti-(1–3) (1–4)-β-glucan], rabbit polyclonal sera against 5-*O*-(*trans*-feruloyl)-L-arabinose (anti-5-O-Fer Ara), and mannan (anti-mannan), and rat monoclonal antibodies against pectic epitopes (JIM7, LM5, and LM6), xyloglucan epitope (LM15), and crystalline cellulose-binding module 3a (CBM3a). The primary references for the generation of the affinity probes as the epitopes recognized are given Table 1.

Nitrogen content

The amount of protein was determined according to the Kjeldahl method using a nitrogen–protein conversion factor of 5.7 (Mosse, 1990).

Table 1. Antibodies and the carbohydrate-binding module used as molecular probes to detect cell wall polysaccharides in *B. distachyon* cross-sections

Antibody/CBM	Antigen/epitope/ligand	References	Availability
(1–3) (1–4)-β-D-glucan	Linear (1–3) (1–4)-β-D-oligosaccharide segment	Meikle *et al.* (1994)	Biosupplies Australia (http://www.biosupplies.com.au)
Anti-AX1	Unsubstituted or low substituted xylan	Guillon *et al.* (2004)	INRA-Anger-Nantes, France
Anti-5-O-Fer-Ara	Highly specific for 5-*O*-(*trans*-feruloyl)-L-arabinose	Philippe *et al.* (2007)	INRA-Anger-Nantes, France
JIM7	Partially methyl-esterified homogalcturonan epitope	Knox *et al.* (1990), Clausen *et al.* (2003)	PlantProbes (http://www.plantprobes.net)
LM5	(1→4)-β-D galactan	Jones *et al.* (1987)	PlantProbes (http://www.plantprobes.net)
LM6	(1–5)-α-L-arabinan	Willats *et al.* (1998)	PlantProbes (http://www.plantprobes.net)
LM15	XXXG heptasaccharides from tamarind seed xyloglucan	Marcus *et al.* (2008)	PlantProbes (http://www.plantprobes.net)
Anti-mannan	(1–4)-β-linked mannosyl residues present within mannan, glucomann, and galactomannan	Handford *et al.* (2003)	Cambridge University, P. Duprée
CBM3a	Cellulose	Blake *et al.* (2006)	PlantProbes (http://www.plantprobes.net)

Polysaccharide analysis

Seed samples were hand dissected and the endosperm separated from the outer tissues. The whole grain as the endosperm and outer layers was ground in liquid nitrogen. Small sugars in the samples (glucose, sucrose, etc.) were removed using ethanol solutions. Briefly, 50 mg of ground tissue was treated with 1 ml of 80% ethanol in a boiling water bath for 30 min. The supernatant was removed after centrifugation at 10 000 rpm for 5 min then the residue was treated with 1 ml of 80% ethanol in a boiling water bath for 10 min. After centrifugation, the pellet was successively washed with 1 ml of 80% ethanol and 1 ml of 96% ethanol, and dried in an oven at 40 °C overnight. Individual neutral sugar and uronic acid analyses were performed as previously described (Saulnier *et al.*, 1995).

Starch and (1–3) (1–4)-β-glucan were analysed according to AOAC procedures [starch, AOAC method 996.11; (1–3) (1–4)-β-glucan, AOAC method 995.16] with a modification for the quantification of glucose using high-performance anion exchange chromatography (HPAEC) instead of an enzymatic kit.

Phenolic acid analysis

Ester-linked phenolic acids were saponified at 35 °C in 2 N sodium hydroxide and extracted with diethylether. The phenolic acids were quantified by reversed phase-HPLC as previously described (Barron *et al.*, 2007). The ferulic acid monomer content was calculated from the amount of *cis*- and *trans*-ferulic acids. The ferulic acid dehydrodimer content was assessed by adding the appropriate amounts of (8-O-4'), (8-5'), 8-5' benzofuran, and 5-5' forms.

Enzymatic fingerprinting

Ethanol-pre-treated ground samples (8 mg) were suspended in water (0.32 ml) and digested overnight at 40 °C under continuous stirring, using a lichenase solution (0.08 ml, 5 U) (Ordaz-Ortiz *et al.*, 2005; Saulnier *et al.*, 2009). A 2 ml aliquot of 95% ethanol was added to the reaction mixture and kept at 4 °C for 1 h. The mixture was then centrifuged (10 000 *g*, 10 min) and the pellet was washed twice with 1 ml of 80% ethanol and dried at 40 °C. The pellet was submitted to a second enzymatic degradation with lichenase under the same conditions. The lichenase residue was isolated as described above. The two ethanol supernatants were combined and evaporated. The resulting dried material was dissolved in water (0.4 ml). The lichenase residue was dispersed in water (0.32 ml) and digested overnight at 40 °C under stirring with endoxylanase (0.08 ml, 5 U). The reaction mixture was boiled for 10 min to inactivate the enzyme. After cooling, the reaction mixture was centrifuged (10 000 *g*, 15 min) and the supernatant was recovered.

The lichenase (1/100 dilution in ultrapure water) and endoxylanase (no dilution) supernatants were analysed by HPAEC. The samples were injected (10 µl aliquots) into a Carbopac PA-200 (5×250 mm) analytical column (Dionex, http://www.dionex.com.; temperature, 25 °C; flow rate, 0.4 ml min^{-1}). Gluco oligosaccharides (GOS) and arabino-xylo oligosaccharides were separated by elution using ultrapure water (A), 1 M NaOAc (B), and 0.5 M NaOH (C) solutions. The elution conditions were: 0 min (A, 60%; C, 40%), 30 min (A, 43%; B, 17%; C, 40%), 35 min (A, 35%; B, 25%; C, 40%), 36 min (A, 20%; B, 40% C, 40%), 38 min (A, 20%; B, 40%; C, 40%), and 39–65 min (A, 60%; C, 40%). A pulse amperometric detector (TSP EC2000, http://www.thermo.com) was used for the detection and quantification of peaks.

Sample preparation for light and infrared microspectroscopy

Transverse sections sampled from half grains were transferred into plastic molds, fixed in formalin for 24 h at 20 °C, and processed for paraffin inclusion as described by Jamme *et al.* (2008). Microtome sections of 6–8 µm (Microm HM 340E, www.thermo.com) were deposited onto glass slides pre-treated with VectaBond (British BioCell International, www.britishbiocell.co.uk) for light microscopy or ZnS windows for infrared microspectroscopy. The paraffin was removed using Histochoice clearing agent (Sigma-Aldrich, http://www.sigmaaldrich.com). Some sections were pre-treated with lichenase (Megazyme, www.megazyme.com, 5 U ml^{-1} in water for 2 h at 40 °C) in order to remove (1–3) (1–4)-β-glucan prior to examination by infrared microspectroscopy.

Sample preparation for light and transmission electron microscopy

Grains from which the lemma and palea were removed were hydrated overnight at 4 °C in a wet chamber. Small pieces of hydrated samples were taken from the equatorial region of grains. They were fixed overnight at 4 °C in a mixture of 3% (w/v) paraformaldehyde and 0.5% (v/v) glutaraldehyde in 0.1 M phosphate buffer (pH 7.2). Fixed samples were rinsed using buffer and de-ionized water prior to dehydration in 30, 50, 70, 85, 95, and 100% ethanol solutions. Samples were successively impregnated with 80/20, 60/40, 40/60, 20/80, and 100/100 (v/v) ethanol/London Resin White (http://www.2spi.com). The impregnated samples were then embedded in gelatin capsules and polymerized for 24 h at 55 °C.

For light microscopy, 1 µm thick resin sections were collected on multiwell glass slides pre-treated with Vectabond (British BioCell International, www.britishbiocell.co.uk). Ultrathin sections (80–100 nm) for electron microscopy were collected on nickel grids.

Fourier transform infrared (FT-IR) microspectroscopy

Infrared spectra of grain cell walls were recorded by taking advantage of the brightness of a synchrotron source (SOLEIL, SMIS beamline, Gif sur Yvette, France). The average current in the storage ring was ~220 mA. The infrared spectral data were recorded using a NICOLET 5700 FT-IR spectrometer (Thermo Fisher Scientific, www.Thermo.com) coupled to a Continuum XL microscope (Thermo Fisher Scientific, www.Thermo.com). The microscope was equipped with a motorized sample stage and a liquid nitrogen-cooled mercury cadmium telluride (MCT-A) detector (50 μm). It operated in a confocal mode, using a ×32 infinity-corrected Schwarzschild objective (NA=0.85) and a matching ×32 condenser. All spectra were obtained using a double path single masking aperture size of 8 μm×8 μm. The spectra were collected in the 1800–800 cm^{-1} infrared range at a spectral resolution of 8 cm^{-1} with 128 co-added scans.

All infrared spectra were pre-processed and submitted to multivariate data analysis (The Unscrambler, CAMO Process AS, www.camo.com). Spectral data were first baseline corrected and unit vector normalized. Second derivatives of the spectral data were assessed (9-point Savitzky–Golay filter) to enhance the resolution of the absorption bands.

The second derivative infrared spectra pre-multiplied by –1 were analysed by applying principal component analysis. The computation of principal components was based on the non-linear iterative projections by alternating least-squares (NIPALS) algorithm. While the score plots allowed a comparison of the infrared spectra, the corresponding loading plots revealed the main characteristic absorption bands.

Light microscopy

All the semi-thin sections (1 μm thick) were observed with a Leica DMRD microscope (Leica, www.leica-microsystems.com). The sections were stained with 0.02 mol l^{-1} iodine for 2 min, washed with water, and stained with fast green (1% in ethanol) for 5 min to observe starch and intracellular proteins. They were extensively rinsed with water before examination on a microscope: bright field or fluorescence (λexcitation, 530–595 nm band-pass filter, and λemission >615 nm) modes.

The cellular structure was visualized by exploiting the native primary fluorescence of cell walls when exciting in UV. A 340–380 nm band-pass filter was used as excitation light, the fluorescence being detected above 425 nm. The microstructure of the grain outer layers was examined using interferential contrast.

Immunolabelling

Sections were successively incubated at room temperature in a blocking solution [3% (w/v) bovine serum albumin (BSA), 0.1 M Na-phosphate buffer saline (PBS), pH 7.2] for 30 min and in solutions containing primary antibodies for 1 h. The dilutions of the antibodies in PBS containing 1% (w/v) BSA and 0.05% (w/v) Tween-20 were: 1:20 for anti-AX1, 1:100 for anti-(1–3) (1–4)-β-glucan, 1:1000 for anti-5-O-Fer-Ara, 1:10 for JIM7, LM5, LM6, and LM15, and 1:1500 for anti-mannan antibodies. The sections extensively washed with buffer were incubated for 1 h in a solution containing the secondary antibody at a dilution of 1:20 (v/v). While the goat anti-mouse IgG was used for anti-AX1 and anti-(1–3) (1–4)-β-glucan antibodies, the goat anti-rabbit IgG conjugated with 1 nm colloidal gold complexes (Aurion, www.aurion.nl) was applied to anti-5-O-Fer-Ara and anti-mannan antibodies. The sections were washed with PBS and water. The gold particles were intensified by homogenous deposition of metallic silver (Aurion, www.aurion.nl).

For immunofluorescence labelling, the sections were treated following the same procedure as that described above but using Alexa 546-conjugated secondary antibody (Molecular Probes, www.invitrogen.com) diluted in PBS [1:100 (v/v)].

Histidine-tagged CBM3a

Sections were successively incubated at room temperature in blocking solution [3% (w/v) BSA, 0.1 M PBS, pH 7.2] for 30 min and in CBM3a solution (PlantProbes, www.plantprobes.net) for 1 h. The 1:500 CBM3a solution was prepared in PBS containing 1% (w/v) BSA and 0.05% (w/v) Tween-20. After washing, the sections were incubated for 1 h in a solution of 1:300 anti-histidine (Sigma H-1029) diluted in the same buffer. Thereafter, the sections were washed with buffer, incubated for 1 h in the presence of the secondary antibody conjugated with 1 nm colloidal gold particles [1:20 (v/v)], and washed again. Finally, the gold particles were silver enhanced as described above.

For fluorescence labelling, the sections were treated as described above, using the Alexa 546–secondary antibody conjugates (Molecular Probes, www.invitrogen.com) diluted in 1:100 buffer.

To remove (1–3) (1–4)-β-glucan and observe the presence of AX, cellulose, pectin, mannan, and xyloglucan in cell walls, sections were pre-treated with lichenase. The pre-treatment involved incubation of the sections with 50 μl of lichenase (4 μg ml^{-1}, Megazyme, I) for 2 h at 38 °C. The sections were then rinsed thoroughly with de-ionized water.

For transmission electron microscopy observations, the sections were counterstained with 2% uranyl acetate and examined on a JEOL 1230 TEM (JEOL, http://www.jeol.com, accelerating voltage of 80 kV).

For light microscopy observations, the sections were examined with a Leica DMRD microscope equipped with epifluorescence.

To assess the non-specific adsorptions of the secondary antibodies, different controls were performed: (i) use of pre-immune serum instead of the polyclonal 5-O-Fer-Ara antibody; and (ii) omission of the primary monoclonal antibodies and CBM3a.

Results

Grain anatomy

The *B. distachyon* grain is enclosed with a palea and lemma which provide protection during development. Its shape is that of a typical caryopse (Fig. 1A); however, it is more pointed and slender than wheat or barley grains. The crease on the ventral side is less re-entrant than in wheat grain (Fig. 1B). The main tissue of the grain is the endosperm, which accounts for 75% of the total de-hulled grain weight. It comprises the aleurone tissue consisting of two or three cell layers and the storage endosperm (Fig. 1B–D). The aleurone cells are relatively small in comparison with those observed in wheat. They are rather cubic in shape and show thick cell walls. The content of the aleurone cells appears to be very dense (Fig. 1D). The storage endosperm consists of cells with very thick walls, making it quite distinct from the storage endosperm of other cereals (Fig. 1C, D). Starch granules surrounded by protein bodies appear concentrated at the periphery of the cells (Fig. 1C, D). The outer tissues are made up of the nucellus layer, the seed coat, and the pericarp (Fig. 1E). The remnants of the nucellus consist of squashed empty cells, the thickness of which is irregular and thin near to the dorsal side. The seed coat that envelops the nucellus epidermis is made up of two cellular layers. The pericarp appears as a multilayered structure composed of squashed cells.

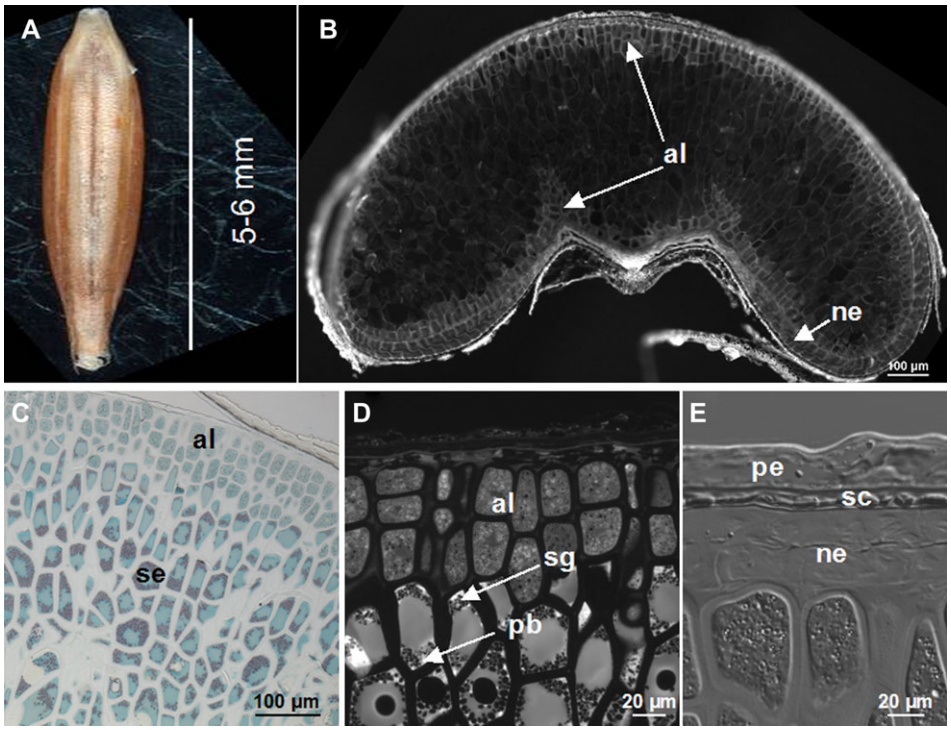

Fig. 1. Image of a whole dehulled *B. distachyon* grain (A) and micrographs of dehulled grain cross-sections (B–E). (B) Primary fluorescence of a paraffin-embedded grain. Excitation light, 340–380 nm band-pass filter; emission light, >425 nm. (C and D) A resin-embedded grain stained with fast green and iodine, showing the aleurone layer (al) and storage endosperm (se). (C) Bright field micrograph; (D) fluorescence micrograph, higher magnification showing the localization of proteins bodies (pb) around starch granules (sg). (E) An interferential contrast micrograph of the outer layers of a paraffin-embedded grain. The outer layer consists of the nucellus epidermis (ne), the seed coat (sc), and the pericarp (pe).

Protein and carbohydrate contents in mature grain

Protein in whole grain accounts for 17% of dry matter. The neutral sugars and uronic acid contents were determined on alcohol-insoluble material prepared from whole grain and isolated tissues (outer layers and endosperm) (Fig. 2). The results are reported in Table 2. The polysaccharides account for 60, 59, and 72% of the whole grain, endosperm, and outer layers, respectively. Glucose is the main sugar detected in the endosperm and outer layers. Arabinose, xylose, and uronic acids occur in significant amounts, while galactose and mannose are minor components. The major part of glucose comes from (1–3) (1–4)-β-glucan found in cell walls (74% of the total glucose in the endosperm). A smaller amount of glucose (12% of the endosperm total glucose) arises from starch. The outer layers are devoid of starch. It is noteworthy that (1–3) (1–4)-β-glucans are found in quite high amounts in the outer layers, accounting for 67% of total glucose.

Fine structure of endosperm (1–3) (1–4)-β-glucan and arabinoxylan

AX and (1–3) (1–4)-β-glucan are key polymers in *B. distachyon* endosperm. Their fine structures were studied by enzymatic fingerprinting, using lichenase and endoxylanase.

Lichenase is a specific *endo* (1–3) (1–4)-β-D-glucan 4-glucanohydrolase that cleaves only (1–4)-β-glucosidic linkages of a three-substituted unit. Lichenase is reported to make (1–3) (1–4)-β-glucan of cereal grains soluble, resulting in GOS. The GOS obtained are mainly 3-*O*-β-cellobiosyl-D-glucose (BG_3), 3-*O*-β-cellotriosyl-D-glucose (BG_4), and oligosaccharides of a higher degree of polymerization (DP5–9) (Tosh *et al.*, 2004; Lazaridou *et al.*, 2007). In *B. distachyon* grains, BG_3 and BG_4 represent 83.2% and 14.2% of the total GOS peaks, respectively (Fig. 3A). GOS of DP5 only accounts for 2.6% (Fig. 3A). The ratio of tri- to tetrasaccharides is significantly higher in *B. distachyon* (5.9) than in wheat (3.7–4.5), barley (2.3–3), and oat (2.3–1.5) (Tosh *et al.*, 2004; Lazaridou and Biliaderis, 2007).

About 20% of xylose is released from the endosperm as water-soluble polymers during lichenase treatment. Therefore, lichenase supernatants were added with ethanol, in order to recover water-soluble xylan in the lichenase residue. The grain and endosperm residues obtained after two successive lichenase treatments were submitted to endoxylanase degradation. The endoxylanase released ~55% and 65% of total xylose from grain and endosperm, respectively. The xylo-oligosaccharides obtained are shown in Fig. 3B. The *B. distachyon* chromatograms were compared with the chromatogram of wheat endosperm water extract obtained after the combined action of lichenase and endoxylanase (Fig. 3C). Despite the two sequential lichenase treatments and the extensive washing of the residue, some GOS peaks are still detected on the chromatogram of

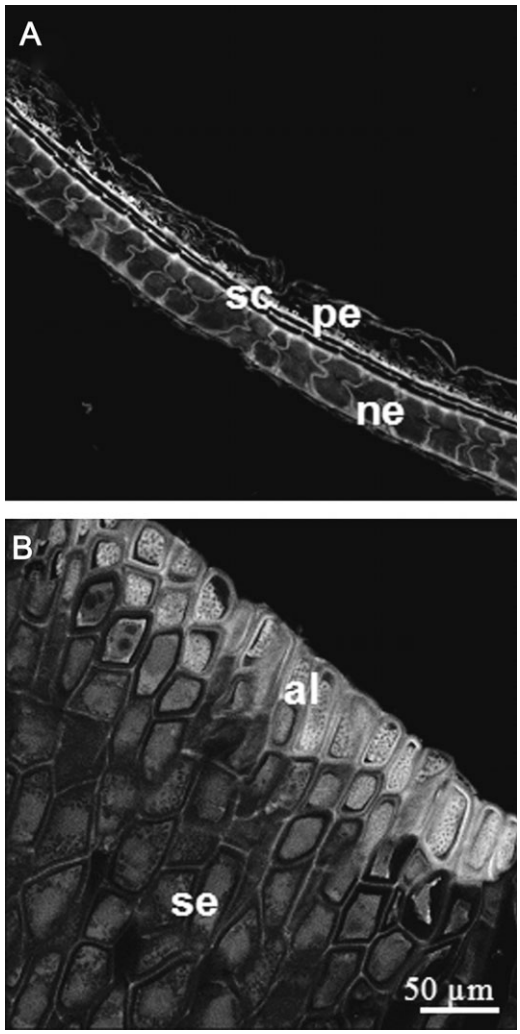

Fig. 2. Fluorescence micrographs of hand-dissected grain tissues. Outer layers (A) and endosperm (B). Excitation light, 340–380 nm band-pass filter; emission light, >425 nm.

the endoxylanase hydrosylates (mainly BG_3 and BG_4). The presence of residual BG_3 and BG_4 is not due to an incomplete digestion of (1–3) (1–4)-β-D-glucan by lichenase or to another activity of the endoxylanase. The endoxylanase used is free from any activity on (1–3) (1–4)-β-D-glucan. This was checked on water-soluble (1–3) (1–4)-β-D-glucan from barley and wheat. No BG_3 or BG_4 peaks were detected in the ethanol washings performed after lichenase treatment. The presence of BG_3 and BG_4 in the xylanase hydrolysate is presumed to be due to their higher solubility in water.

Xylose (X) xylobiose (XX) and the arabino-xylo-oligosaccharides XA^3X, XA^3XX, $XA^{2+3}XX$, XA^3A^3XX, XA^3XA^3XX, $XA^3A^{2+3}XX$, and $XA^{2+3}A^{2+3}XX$ are the main oligosaccharides (for nomenclature, see Faure *et al.*, 2009) found in the endoxylanase hydrolysate. These oligosaccharides are detected in wheat endosperm together with the unknown oligosaccharides UX2, UX4, and UX6. In addition, some oligosaccharides eluting at 12.55 (Ubra1), 15.08 (Ubra2), and 23.33 min (Ubra3), quite abundant in *Brachypodium* xylan hydrolysate, are absent in wheat. These oligosaccharides probably reveal some specific structural features that need further studies for identification.

Table 2. Sugar composition (mg 100 mg^{-1}) of the alcohol-insoluble material prepared from whole grain and isolated grain tissues

	Whole grain	Endosperm	Outer layers
Arabinose[a]	2.2	1.4	3.7
Xylose	2.5	1.3	5.5
Mannose	0.2	0.1	0.2
Galactose	0.5	0.5	0.4
Glucose	54.8	55.4	62.4
Galacturonic acid[b]	1.3	0.9	2.1
Glucuronic acid	0.2	Trace	0.2
Total	60.1	58.6	72.1
Starch[c]	6.4	6.9	0.5
(1–3) (1–4)-β-glucan[c]	42.4	41.2	41.8
Arabinoxylan[d]	4.7	2.7	9.2
Cellulose[e]	6.0	7.3	20.1

[a] Individual neutral sugars determined by gas–liquid chromatography of alditol acetates.
[b] Uronic acids determined by a colorimetric method (Saulnier *et al.*, 1995).
[c] Starch and (1–3) (1–4)-β-glucan determined by enzymatic methods (AOAC methods 996.11 and 995.16, respectively).
[d] Arabinoxylan estimated as the sum of arabinose and xylose.
[e] Cellulose estimated by the difference between total glucose determined by gas–liquid chromatography of alditol acetates, and starch + (1–3) (1–4)-β-glucan contents determined by enzymatic methods. No xyloglucan was detected by either enzymatic fingerprinting or immunolabelling.

Xylan from *B. distachyon* and wheat endosperms shares common structural features (Saulnier *et al.*, 2009). However, xylan of *B. distachyon* contains a higher proportion of di-substitution, and some structural features seem to be specific.

Phenolic acids in mature grain

The hydroxycinnamate content of cell walls in whole grains and isolated tissues was determined (Table 3).

As observed for cereal grains, the main hydroxycinnamic acids encountered in whole *B. distachyon* grain are ferulic acid (1.63 µg mg^{-1}), dehydrodimers of ferulic acid (0.2 µg mg^{-1}), and *para*-coumaric acid (0.09 µg mg^{-1}). The phenolic acid amounts in *B. distachyon* endosperm are in the same range as those observed for other cereal grains (Li *et al.*, 2008). Their localization within the grain is comparable with that of others cereals, the outer layers being more particularly enriched (Table 3). Taking the ratio of phenol to arabinose and xylose units into account, AX in *B. distachyon* appears to be highly feruloylated, regardless of the tissue (Miller *et al.*, 1995; Barron *et al.*, 2007; Lazaridou *et al.*, 2008). Both the endosperm and outer layers have a quite low molar ratio of xylose to dehydromers of ferulic acid (420 and 287, respectively), suggesting a high degree of AX cross-linking (intermolecular links). This has to be further demonstrated as ferulate dimers could link one part of AX to another part of the molecule (intramolecular links).

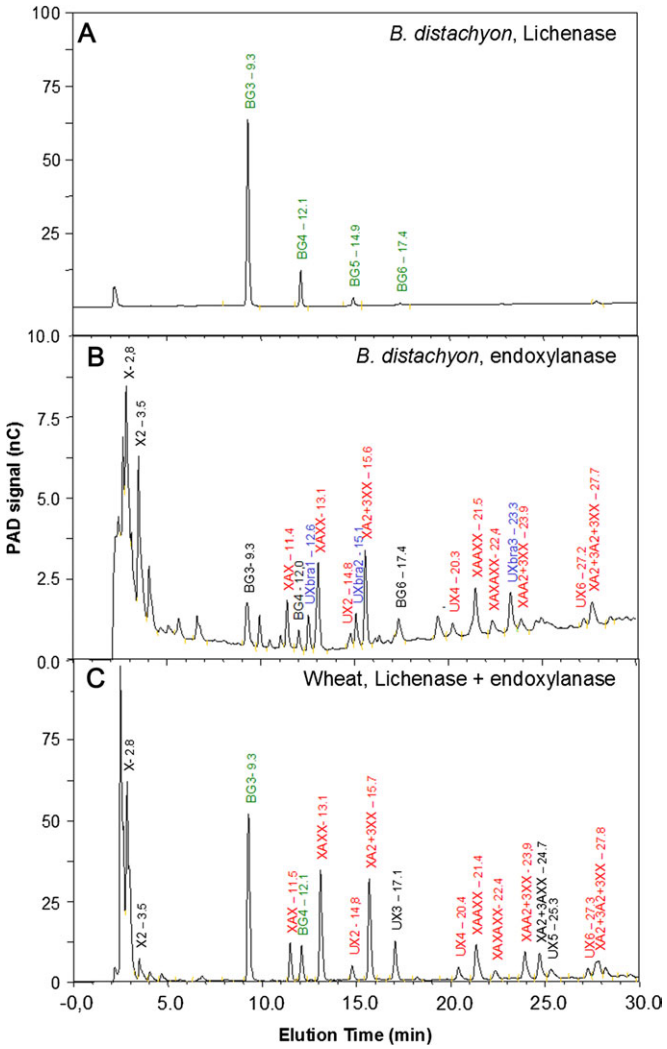

Fig. 3. HPAEC analysis of oligosaccharides produced by enzyme fingerprinting of endosperm cell walls. (A) Oligosaccharides released from (1–3) (1–4)-β-glucans by digestion with lichenase. (B) Oligosaccharides released from xylans by digestion with endoxylanase after lichenase treatment. (C) Oligosaccharides released from wheat endoperm water-soluble extract by combined treatment with lichenase and xylanase.

Analysis of endosperm cell wall by FT-IR microspectroscopy

FT-IR microspectroscopy has been shown to be powerful in the investigation of *in situ* cell wall composition (Jamme *et al.*, 2008; Saulnier *et al.*, 2009). Although a precise assignment of polysaccharide absorption bands remains difficult, each polysaccharide presents specific peaks in the 1200–800 cm^{-1} infrared range. (1–3) (1–4)-β-glucan is characterized by infrared absorption bands at ~1155, 1070, and 1030 cm^{-1}. Cellulose differs from (1–3) (1–4)-β-glucan by absorption bands at 1160, 1060, and 1030 cm^{-1}. The main absorption band for AX is observed at ~1040 cm^{-1}, with shoulders at 1070 cm^{-1} and 985 cm^{-1} (Robert *et al.*, 2005). In the present study, FT-IR microspectroscopy was applied to explore the cell wall composition of the storage endosperm and aleurone layers. The synchrotron source, thanks to its brightness, allows a confocal configuration to be set up at an aperture size consistent with cell wall dimensions in *B. distachyon* endosperm. It allows the acquisition of cell wall spectra free of cell contamination.

Table 3. Phenolic acid composition (μg mg^{-1} of tissue) of whole grain and isolated tissues

	Whole grain	Endosperm	Outer layers
Para-coumaric acid	0.09	0.02	0.54
Sinapic acid	0.01	ND	ND
Ferulic acid (monomer)	1.63	0.74	4.34
Dehydromers of ferulic acid	0.20	0.09	0.56
Ferulic acid trimer	0.03	0.01	0.13
Xylose/ferulic acid dimer molar ratio	365	422	287
% Phenol/(ara+xyl)	4.2	3.0	6.1

Ferulic acid (monomer) values were calculated by summing *cis*-ferulic acid and *trans*-ferulic acid. Dehydromers of ferulic acid values were calculated by summing the contents of 8-5', 8-5' benzo, 8-*O*-4' and 5-5' diferulates. Ferulic acid trimer values were 4-*O*-8', 5'-5'' ferulic acid dehydrotrimer. The values for the xylose to ferulic acid dimer ratio were calculated by using a molecular weight for the ferulic acid dimer of 386 Da. ND, not detected.

Cell wall infrared spectra of the aleurone layer and storage endosperm recorded in the 1200–800 cm^{-1} range are given Fig. 4A. The main absorbance bands observed at 1150, 1070, 1030, and 890 cm^{-1} indicate that cell walls are enriched in (1–3) (1–4)-β-glucan. The cell wall infrared spectra, after lichenase treatment, exhibit wide absorption bands with a maximum characteristic of AX at ~1045 cm^{-1} (Fig. 4B). Principal component analysis was applied to the second derivative spectral data of cell walls pre-treated with lichenase. The first two principal components take 65% and 10% of the total variance into account. Principal component 1 discriminates the infrared spectra of the aleurone and storage endosperm (Fig. 4C). The loading plot of the first principal component (Fig. 4D) reveals negative peaks at ~1160 cm^{-1} and 1060 cm^{-1}, indicating that the cell walls of the storage endosperm are richer in cellulose than in the aleurone layer.

(1–3) (1–4)-β-glucan, AX, and cellulose are therefore the main polysaccharides encountered in the cell walls of both the aleurone and storage endosperm of *B. distachyon*.

Immunolocalization of endosperm cell wall polysaccharides

The results obtained by FT-IR microspectroscopy of the distribution of the polysaccharides within the endosperm were compared with those observed using immunogold localization [(1–3) (1–4)-β-glucan, AX, and cellulose]. The distribution of ferulic acid was investigated using the anti-5-O-Fer-Ara antibody. While the presence of pectin and mannan was ascertained using pectin and anti-mannan antibodies, the occurrence of xyloglucan was investigated using LM15.

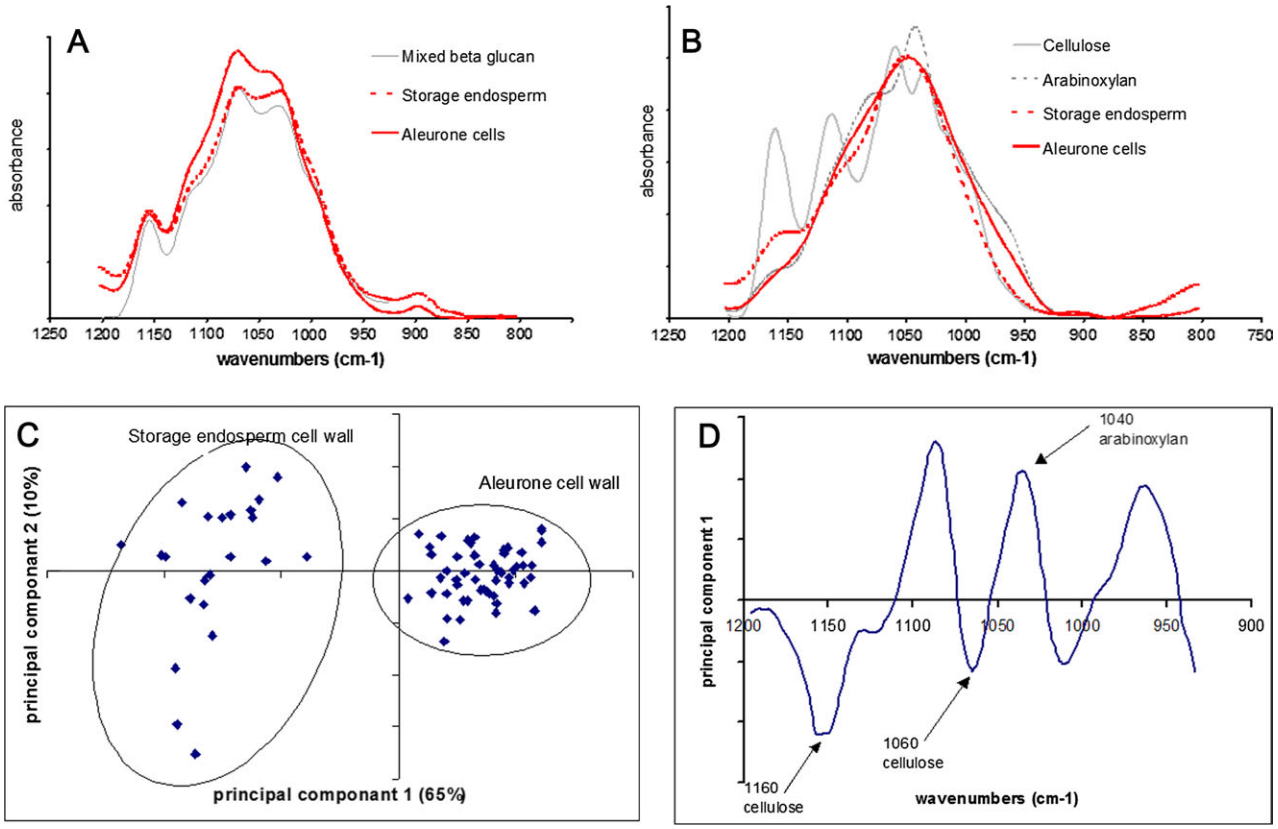

Fig. 4. Analysis of endosperm cell wall by FT-IR microspectroscopy. (A) Infrared spectra of aleurone and storage endosperm cell walls over the polysaccharide range (1800–800 cm^{-1}). (B) Infrared spectra of aleurone and storage endosperm cell walls over the polysaccharide range (1800–800 cm^{-1}) after pre-treatment with lichenase. (C and D) Principal component analysis (PCA) applied to FT-IR spectra of aleurone and storage endosperm cells walls pre-treated with lichenase. (C) Similarity map from PCA of FT-IR spectra obtained for the aleurone and storage endosperm cell walls. (D) Spectral patterns obtained from the first PCA loading (PC1), showing influent wave numbers for the discrimination of aleurone and storage endosperm cell walls.

(1–3) (1–4)-β-glucan is abundant in both the aleurone and endosperm cell walls (Fig. 5A). It is localized throughout the primary wall, except in the middle lamella (Fig. 5B, C) and cell junction zones. In the aleurone layer, intense labelling is observed near to the plasma membrane (Fig. 5B).

In the absence of lichenase pre-treatment, AX is visualized in the middle lamella and cell junction zones of both the aleurone and storage endosperm cell walls (Fig. 6A–E). Lichenase pre-treatment of grain sections increases the labelling (Fig. 6F–J). While AX is uniformly distributed throughout the primary walls of the aleurone layer, it only appears in the middle lamella and junction zones of the cells observed in the storage endosperm. The anti-5-O-Fer-Ara antibody labels the aleurone cell walls across their width, after lichenase pre-treatment (Fig. 7A). The cell junction zones are strongly labelled (Fig. 7B). The labelling of storage endosperm cell walls is predominantly localized to the junction zone and the region close to the middle lamella (Fig. 7C, D).

Cellulose, mannan, and pectin in cell walls were visualized only after removal of the (1–3) (1–4)-β-glucan by lichenase pre-treatment. No labelling is observed with LM15. The cellulose labelling is distributed throughout the walls, except in the middle lamella and cell junction zones (Fig. 8). The density of the labelling appears more intense in the cell walls of the storage endosperm than in the cell walls of the aleurone layer (Fig. 8A–C). In contrast to the aleurone cell walls, the labelling of the storage endosperm walls is not uniformly distributed (Fig. 8C).

The potential presence of homogalacturonan (HG) and rhamnogalacturonan (RGI) in cell walls was investigated using pectin antibodies (RGI, LM5 and LM6 antibodies; HG, JIM7). While the cell walls of the storage endosperm are labelled with JIM7 (Fig. 9A, C), the walls of the aleurone cells are poorly labelled (Fig. 9A, B). No labelling is noticed with LM6. The galactan epitope (LM5) detected in the aleurone cell walls (Fig. 9D, E), reveals that galactan is mostly found in the region close to the plasma membrane. LM5 binds very weakly to the cell walls of the storage endosperm (Fig. 9D, F).

The mannan epitope is less abundant in the cell walls of the aleurone cells than in those of the storage endosperm (Fig. 10A–C). Labelling is not uniform across the storage endosperm cell walls and is absent in the middle lamella (Fig. 10C).

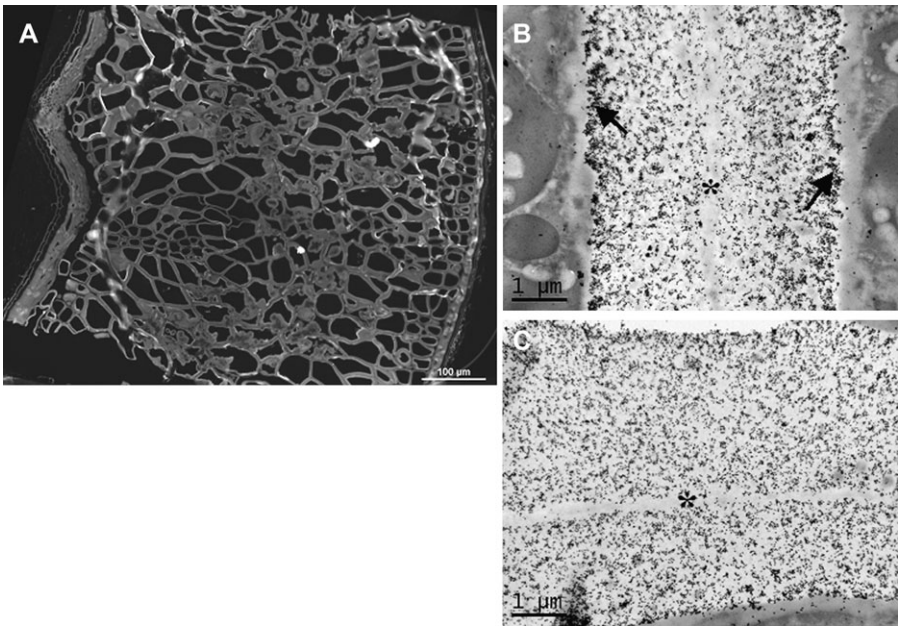

Fig. 5. Fluorescence and transmission electron micrographs of mature endosperm cell walls labelled with antibody to (1–3) (1–4)-β-D-glucans. (A) Immunofluorescence labelling of mature endosperm cell walls. (B) Immunogold labelling of the cell wall between two aleurone cells; note the intense labelling adjacent to the plasma membrane (arrows). (C) Immunogold labelling of the cell wall in the central region of the endosperm. Intense labelling was evenly distributed throughout the wall, except in the middle lamella (*).

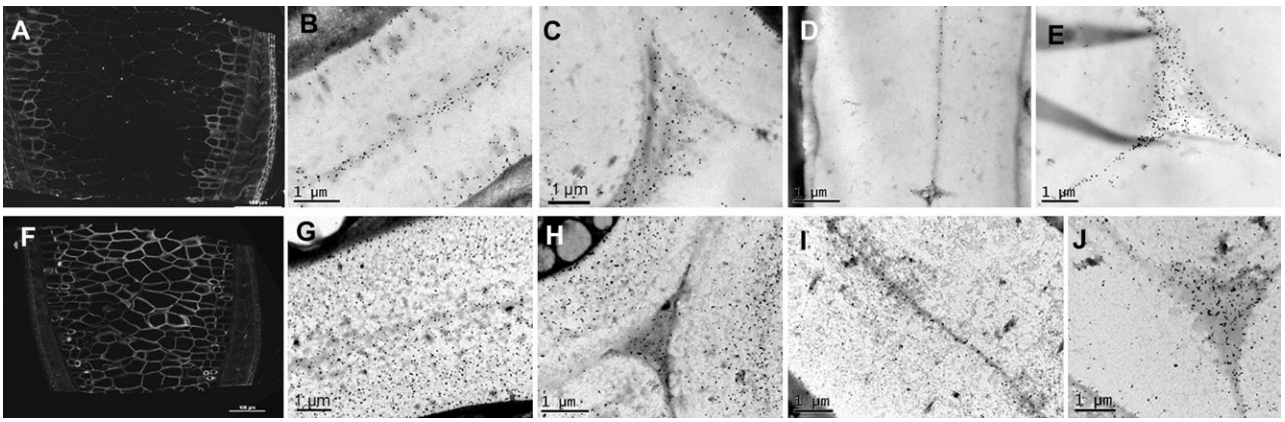

Fig. 6. Fluorescence and transmission electron micrographs of mature endosperm cell walls labelled with antibody to AX. (A–E) Labelling with anti-AX1 antibody without lichenase treatment. (F–J) Labelling with anti-AX1 antibody after lichenase treatment. (A and F) Immunofluorescence labelling of mature endosperm cell walls. (B–E and G–I) Immunogold labelling. (B and G) Cell walls between two aleurone cells. (C and H) Cell junction in the aleurone layer. (D and I) Cell walls in the central region of the endosperm. (E and K) Cell junction in the central region of the endosperm. The AX labelling is more intense after lichenase treatment. In the storage endosperm, labelling is mainly located at cell junctions and in the middle lamella.

Discussion

Grain anatomy and composition

Brachypodium distachyon grains exhibit some specificities from other cereal grains. They, in particular, present a hull of adherent palea and lemma which are removed with difficulty. The cell walls of the storage endosperm are very thick in comparison with those of other cereals. The *B. distachyon* grain is notable for its high content of cell wall polysaccharides. The polysaccharide content reaches up to 60% (w/w) in de-hulled whole grains and to 58% (w/w) in the endosperm. The cell wall polysaccharides in wheat (10–13%), oat (11–13), and barley (15–20%) de-hulled whole grains are substantially lower than in *B. dystachyon* (Oscarsson *et al.*, 1996; Manthey *et al.*, 1999; Antoine *et al.*, 2003; Barron *et al.*, 2007). The protein content of *B. distachyon* grain approaches the highest level encountered in cereal grains. The protein content is close to that measured in oat grains.

The outer layers of *B. distachyon* are characterized by a high content of (1–3) (1–4)-β-glucan and a low level of xylan. They are especially rich in phenolic acids, the

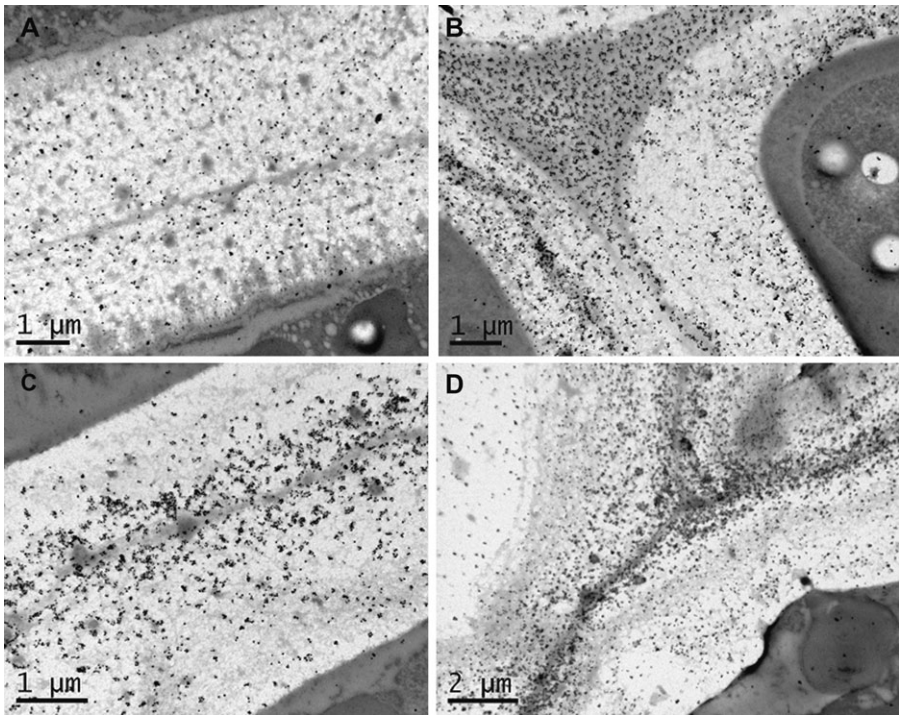

Fig. 7. Transmission electron micrographs of mature endosperm cell walls labelled with anti-5-O-Fer-Ara antibody after lichenase treatment. (A) Cell walls between two aleurone cells. (B) Cell junction in the aleurone layer. (C) Cell walls in the central region of the endosperm. (D) Cell junction in the central region of the endosperm. The epitope 5-O-Fer-Ara accumulates at cell junctions in both storage endosperm and aleurone layers.

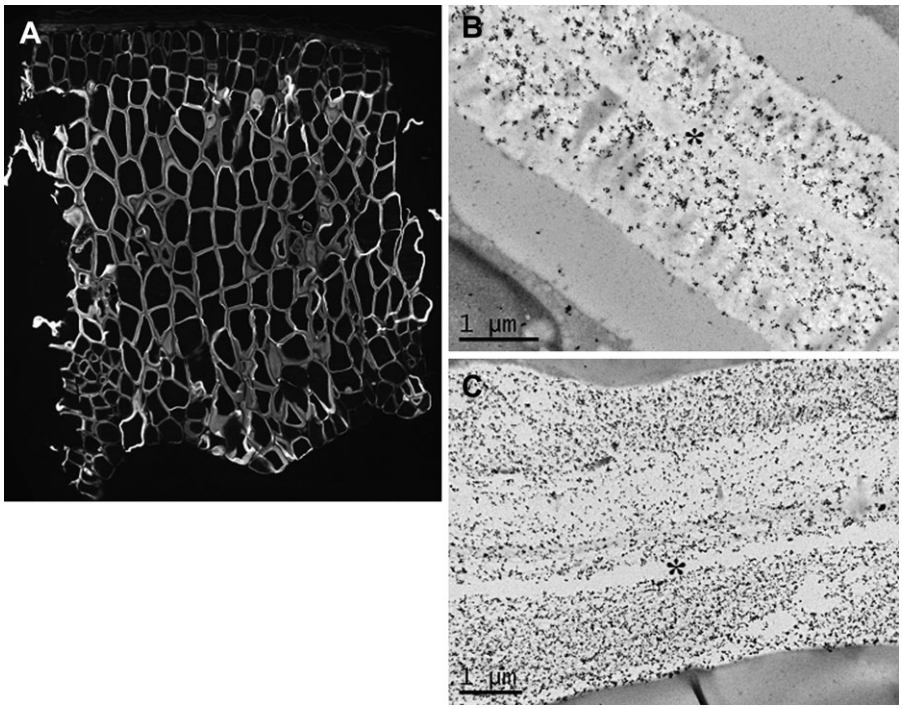

Fig. 8. Fluorescence and transmission electron micrographs of mature endosperm cell walls labelled with His-tagged cellulose-directed CBM after lichenase treatment. (A) Immunofluorescence labelling of mature endosperm cell walls. (B and C) Immunogold labelling. (B) Aleurone layer; (C) storage endosperm. In both aleurone and endosperm cells, immunolabelling is distributed throughout the wall, except in the middle lamella (*). In the storage endosperm, labelling is denser and not homogenous. Cj, cell junction.

dimer/monomer ferulic acid ratio in *B. distachyon* being similar to that obtained for other cereals. Assuming that glucose not arising from (1–3) (1–4)-β-glucan mainly originates from cellulose (Table 2), the cellulose content remains in the range reported for other cereal grains (Antoine *et al.*, 2003).

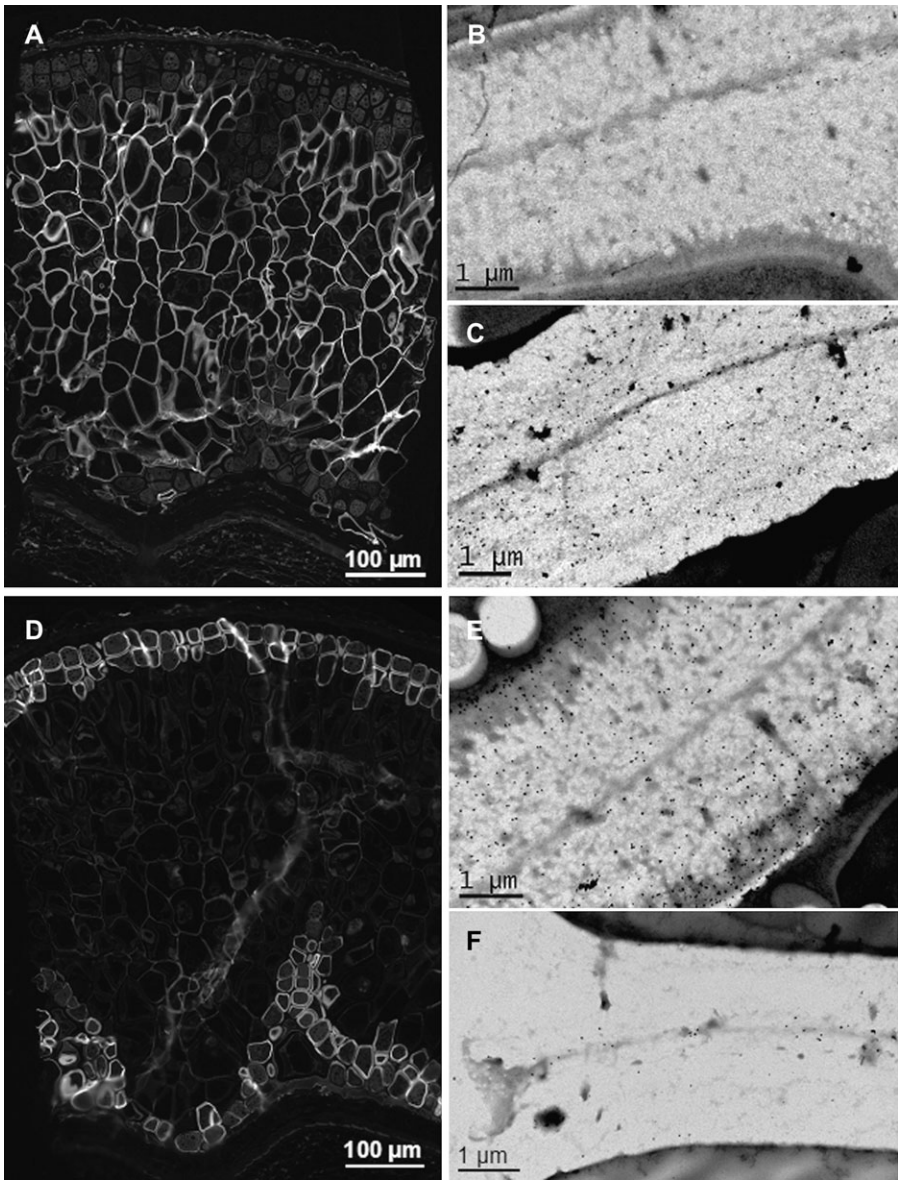

Fig. 9. Immunofluorescence and transmission electron micrographs of mature endosperm cell walls labelled with JIM7 (A–C) and LM5 (D–F) after lichenase treatment. Homogalacturans are detected mainly in the storage endosperm while galactans are found in the aleurone cell walls.

Carbohydrates in B. distachyon *endosperm*

The starch content of the endosperm is low (<10% of that of the whole grain) in comparison with most domesticated cereals (50–70%). Conversely, the amount of (1–3) (1–4)-β-glucan is unusually high. While the proportion of (1–3) (1–4)-β-glucan in the cell walls of *B. distachyon* endosperm amounts to ~80% (w/w), it represents ~75, 70, and 25% (w/w) of the total polysaccharides in barley, oat, and wheat endosperm, respectively (Fincher and Stone, 1986). (1–3) (1–4)-β-glucan is present in high concentrations in both the aleurone and storage endosperm cell walls of *B. distachyon*. An even distribution of (1–3) (1–4)-β-glucan is observed in the storage endosperm, as in barley. At the cell wall scale, (1–3) (1–4)-β-glucan in *B. distachyon* grains is absent from the middle lamella and cell junction zones. In wheat, (1–3) (1–4)-β-glucan is found throughout the cell walls of the aleurone layer, but is restricted in the storage endosperm to regions close to the lumen (Guillon *et al.*, 2004).

The (1–3) (1–4)-β-glucan is found in the cell walls of most members of the Poaceae and of some lower vascular plants such as the horsetails (Trethewey *et al.*, 2005; Fry *et al.*, 2008; Sorensen *et al.*, 2008; Burton and Fincher, 2009). In cereals and grasses, it is found as a minor component in mature vegetative cell walls, but as a major component in mature endosperm cell walls (Buckeridge *et al.*, 2004; Fincher and Stone, 2004). The fine chemical structure of (1–3) (1–4)-β-glucan varies among cereal species (Cui *et al.*, 2000; Tosh *et al.*, 2004; Lazaridou *et al.*, 2007; Izydorczyck and Dexter, 2008). The proportion of 3-*O*-β-cellotriosyl-D-glucose units is higher in *B. distachyon* endosperm than in wheat, barley, and oat endosperm. The function of (1–3)

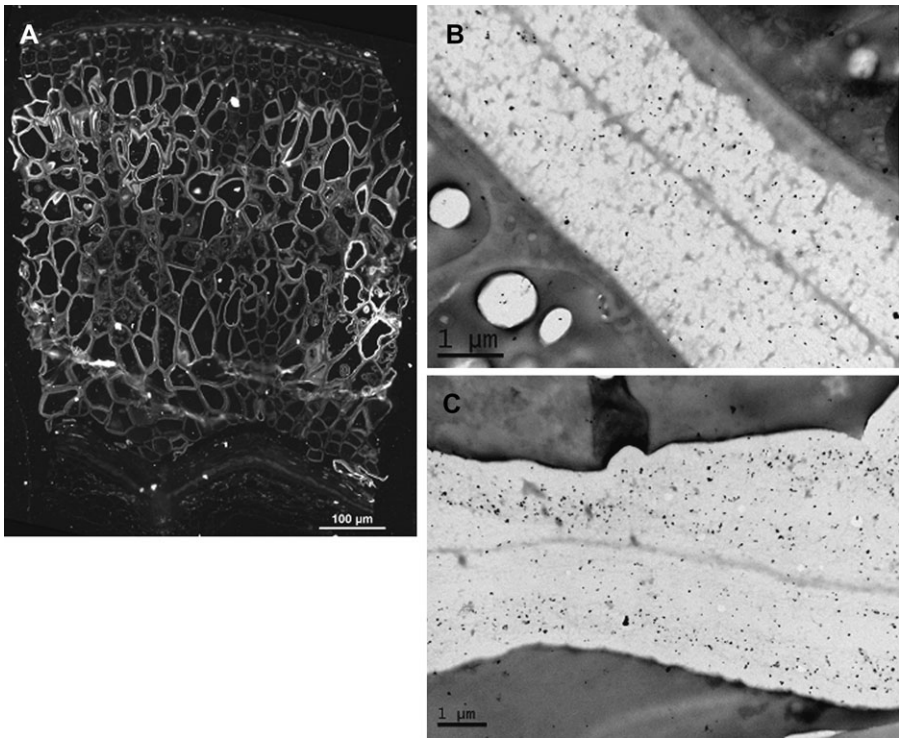

Fig. 10. Fluorescence and transmission electron micrographs of mature endosperm cell walls labelled with anti-mannan antibody after lichenase treatment. (A) Immunofluorescence labelling of mature endosperm cell walls. (B and C) Immunogold labelling. Mannans are detected in higher amounts in storage endosperm cell walls (A, C) compared with aleurone cell walls (B).

(1–4)-β-glucan in cell walls remains to be addressed. In maize, *B. distachyon*, *Hordeum vulgare*, and *Triticum aestivum* coleoptiles, (1–3) (1–4)-β-glucan is synthesized during the rapid phase of elongation. It is degraded when the elongation of the cells ceases (Carpita *et al.*, 2001; Trethewey and Harris, 2002; Buckeridge *et al.*, 2004; Christensen *et al.*, 2009). The presence of (1–3) (1–4)-β-glucan is thought to participate in the control of cell wall extension during growth (Buckeridge *et al.*, 2004). The situation is quite different in the endosperm of cereal grain. (1–3) (1–4)-β-glucan is laid down during the cellularization phase and remains present throughout the development of the endosperm (Philippe *et al.*, 2006; Wilson *et al.*, 2006). It contributes up to 18% of the total glucose stored in domesticated cereal grains (Morall and Briggs, 1978; Buckeridge *et al.*, 2004). In *B. distachyon*, the high amount of (1–3) (1–4)-β-glucan and low starch content suggest that β-glucan has a storage function. Like galactomannan, xyloglucan, and galactan in seeds (Buckeridge *et al.*, 2000, 2004), (1–3) (1–4)-β-glucan in *B. distachyon* grain must be mobilized during germination.

Beside (1–3) (1–4)-β-glucan, *B. distachyon* cell walls of the endosperm contain cellulose and xylan in significant amounts (Table 2). The immunolabelling experiments exclude the presence of xyloglucan but reveal low amounts of pectin and mannan.

Assuming that glucose not arising from (1–3) (1–4)-β-glucan mainly originates from cellulose, cellulose accounts for ~7% in the endosperm cell walls of *B. distachyon*. In most cereal grains except rice, cellulose occurs as a minor component of the endosperm cell wall [2–4% (w/w)] (Fincher and Stone, 1986). Cellulose in the storage endosperm cell walls of *B. distachyon* occurs in higher amounts than in the cell walls of the aleurone layers. In both tissues, cellulose is distributed throughout the wall, except in the middle lamella. Cellulose in *B. distachyon* endosperm may contribute to the maintenance of cell walls.

Both arabinose and xylose only account for 2.7 % (w/w) of the total cell wall sugars. The AX content in *B. distachyon*, wheat, and barley endosperm is similar. The enzymatic fingerprinting reveals that AX in the endosperm of *B. distachyon* has a high proportion of di-substitution.

Considering the ratio of phenol to arabinose and xylose units, AX in *B. distachyon* endosperm cell walls is highly feruloylated (Barron *et al.*, 2007; Lazaridou *et al.*, 2008).

While AX in the storage endosperm is mainly located in the middle lamella and at the cell junction zones, it is distributed throughout the walls of the aleurone cells. In both the storage endosperm and aleurone layer, esterified ferulic acid is abundant at the cell junctions. These results are consistent with the general assumption that feruloylated AXs are involved in the cell wall reinforcement and cohesion of cells through cross-linking via diferulic bridges (Iiyama *et al.*, 1994; Peyron *et al.*, 2001).

The mannan and pectin only account for a few percent of *B. distachyon* endosperm cell walls. The presence of heteromannan in the endosperm cell walls has been reported in other cereals (Fincher and Stone, 1986). In barley

endosperm, Wilson *et al.* (2006) shed some light on their deposition during grain development. They revealed that the hetero-mannan is laid down during the cellularization stage, just after the (1–3) (1–4)-β-glucan deposition (Wilson *et al.*, 2006). Mannan is believed to have the same function as xyloglucan in dicotyledons during cell growth and development.

Except for rice grain, pectic polysaccharides are not present in the cell walls of cereal grain endosperm (Shibuya and Nakane, 1984). In *B. distachyon*, immunolabelling reveals a spatial heterogeneity in the distribution of pectic epitopes. While *B. distachyon* exhibits very low amounts of pectin, dicotyledons are characterized by a high pectin content in their primary cell walls. The structural features of pectic polysaccharides are diverse and highly regulated during cell growth and differentiation (Verhertbruggen and Knox, 2006; Knox, 2008). The pectin present in the middle lamella, and the primary and secondary cell walls plays an important role in the formation of plant cell walls and influences cell wall porosity, surface charge, pH, and ion balance, as well as mechanical properties (Voragen *et al.*, 2009).

Conclusion

As in other cereals, the cell walls of *B. distachyon* grain endosperm mainly contain (1–3) (1–4)-β-glucan and feruloylated AXs. However, cellulose in *B. distachyon* cell walls occurs in significant amounts, in comparison with other cereals. (1–3) (1–4)-β-glucan is the major component of *B. distachyon* seed and this cell wall polysaccharide is the main storage carbohydrate in the grain. This trait distinguishes *B. distachyon* from most of the domesticated cereals. Cell walls are of importance for the growth and development of cereal grains with both structural and storage functions. They are involved in various aspects of grain uses such as in food and feed applications. The fully sequenced genome of *B. distachyon* makes it a good model to investigate cell wall polysaccharide synthesis and function in cereal, in particular (1–3) (1–4)-β-glucan and feruloylated AXs. In addition, *B. distachyon* might provide new insights into the processes involved in the regulation of storage carbohydrate in seeds.

Acknowledgements

We thank M. Goneau (TGU Institut Jean-Pierre Bourgin, INRA Versailles) for providing grains of *B. distachyon*. We gratefully acknowledge the gift of antibodies from Dr P. Duprée (University of Cambridge, UK). We are indebted to S. Daniel for his technical support in isolation of grain tissues, chemical analysis, and enzymatic fingerprinting experiments. A. Putois is thanked for phenolic acid analyses. Synchrotron FT-IR experiments have been performed at the synchrotron SOLEIL on the SMIS beamline in the framework of proposals 20080180 and 99080049.

References

Antoine C, Peyron S, Mabille F, Lapierre C, Bouchet B, Abecassis J, Rouau X. 2003. Individual contribution of grain outer layers and their cell wall structure to the mechanical properties of wheat bran. *Journal of Agricultural and Food Chemistry* **51,** 2026–2033.

Barron C, Surget A, Rouau X. 2007. Relative amounts of tissues in mature wheat (Triticum aestivum L.) grain and their carbohydrate and phenolic acid composition. *Journal of Cereal Science* **45,** 88–96.

Blake AW, McCartney L, Flint JE, Bolam DN, Boraston AB, Gilbert HJ, Knox JP. 2006. Understanding the biological rationale for the diversity of cellulose-directed carbohydrate-binding modules in prokaryotic enzymes. *Journal of Biological Chemistry* **281,** 29321–29329.

Bolot S, Abrouk M, Masood-Quraishi U, Stein N, Messing J, Feuillet C, Salse J. 2009. The 'inner circle' of the cereal genomes. *Current Opinion in Plant Biology* **12,** 119–125.

Buckeridge MS, Pessoa dos Santos H, Tiné MAS. 2000. Mobilisation of storage cell wall polysaccharides in seeds. *Plant Physiology and Biochemistry* **38,** 141–156.

Buckeridge MS, Rayon C, Urbanowicz B, Tiné MAS, Carpita NC. 2004. Mixed (1→3) (1→4)-β-D-glucans of grasses. *Cereal Chemistry* **81,** 115–127.

Burton RA, Fincher GB. 2009. (1,3; 1,4)-β-D-Glucans in cell walls of the Poaceae, lower plants, and fungi: a tale of two linkages. *Molecular Plant* **2,** 873–882.

Catalan P, Ying S, Armstrong L, Draper J, Stace CA. 1995. Molecular phylogeny of the grass genus *Brachypodium* P. Beuav. based on RFLP and RAPD analysis. *Botanical Journal of the Linnean Society* **117,** 263–280.

Carpita NC, Defernez M, Findlay K, Wells B, Shoue DA, Catchpole G, Wilson RH, McCann MC. 2001. Cell wall architecture of the elongating maize coleoptile. *Plant Physiology* **127,** 551–565.

Clausen MH, Willats WGT, Knox JP. 2003. Synthetic methyl hexagalacturonate hapten inhibitors of anti homogalacturonan monoclonal antibodies LM7, JIM5 and JIM7. *Carbohydrate Research* **338,** 1797–1800.

Christensen U, Alonso-Simon A, Scheller HV, William GT, Willats WGT, Harholt J. 2010. Characterization of the primary cell walls of seedlings of *Brachypodium distachyon*—a potential model plant for temperate grasses. *Phytochemistry* **71,** 62–69.

Cui W, Wood PJ, Blackwell B, Nikiforuk J. 2000. Physicochemical properties and structural characterization by two-dimensional NMR spectroscopy of wheat β-D-glucans—comparison with other cereal β-D-glucans. *Carbohydrate Research* **35,** 225–243.

Dervilly G, Saulnier L, Roger P, Thibault JF. 2000. Isolation of homogeneous fractions from wheat water-soluble arabinoxylans. Influence of the structure on their macromolecular characteristics. *Journal of Agricultural and Food Chemistry* **48,** 270–278.

Draper J, Mur LAJ, Jenkins G, Ghosh-Biswas GC, Bablak P, Hasterok R, Routledge APM. 2001. *Brachypodium distachyon*. A new model system for functional genomics in grasses. *Plant Physiology* **127,** 1539–1555.

Doust A. 2007. Architectural evolution and its implications for domestication in grasses. *Annals of Botany* **100,** 941–950.

Faure R, Courtin CM, Delcour JA, *et al*. 2009. A brief and informationally rich naming system for oligosaccharide motifs of heteroxylans found in plant cell walls. *Australian Journal of Chemistry* **62,** 533–537.

Fincher GB, Stone BA. 1986. Cell walls and their components in cereal grain technology. *Advances in Cereal Science and Technology* **8,** 207–295.

Fincher GB, Stone BA. 2004. Chemistry of non starch polysaccharides. In: Wrigley C, Corke H, Walker CE, eds. *Encyclopedia of grain science*. Oxford: Elsevier, 206–223.

Fry SC, Nesselrode BH, Miller JG, Mewburn BR. 2008. Mixed-linkage (1→3) (1→4)-β-D glucan is a major hemicellulsoe of Equisetum (horsetail) cell walls. *New Phytologist* **179,** 104–115.

Garvin DF, Gu YQ, Hasterok R, Hazen SP, Jenkins G, Mockler TC, Mur LA, Vogel PP. 2008. Development of genetic and genomic research resources for *Brachypodium distachyon*, a new model system for grass crop research. *Crop Science* **48**(Supplement 1), S69–S84.

Guillon F, Tranque O, Quillien L, Utille J-P, Ordaz-Ortiz JJ, Saulnier L. 2004. Generation of polyclonal and monoclonal antibodies against arabinoxylans and their use for immunocytochemical localization of arabinoxylans in cell walls of the wheat grain endosperm. *Journal of Cereal Science* **40,** 167–182.

Handford MG, Baldwin TC, Goubet F, Prime TA, Miles J, Yu XL, Dupree P. 2003. Localisation and characterisation of cell wall mannan polysaccharides in *Arabidopsis thaliana. Planta.* **218,** 27–36.

Harholt J, Bach IC, Lind-Bouquin S, Nuna K, Brinch-pedersen H, Holm PB, Scheller H. 2010. Generation of transgenic wheat (*Triticum aestivum* L.) accumulating heterologous endo-xylanase or ferulic esterase in the endosperm. *Plant Biotechnology Journal* **8,** 351–362.

Hasterok R, Draper J, Jenkins G. 2004. Laying the cytotaxonomic foundations of a new model grass, *Brachypodium distachyon* (L.) Beauv. *Plant Physiology* **127,** 1539–1555.

Huo N, Lazo G, Vogel J, You F, *et al*. 2008. The nuclear genome of *Brachpodium distachyon*: analysis of BAC and sequences. *Functional and Integrative Genomics* **8,** 135–147.

Iiyama K, Lam TBT, Stone BA. 1994. Covalent cross-links in the cell wall. *Plant Physiology* **104,** 315–320.

International Brachypodium Initiative. 2010. Genome sequence analysis of the model grass Brachypodium distachyon. *Nature* **463,** 763–768.

Izydorczyk MS, Biliaderis CG. 2007. Arabinoxylans: technologically and nutritionally functional plant polysaccharides. In: Biliaderis CG, Izydorczyk MS, eds. *Functional food carbohydrates*. Boca Raton, FL: CRC Press, Taylor & Francis Group, 249–290.

Izydorczyk MS, Dexter JE. 2008. Barley glucans and arabinoxylans: molecular structure, physicochemical properties, and uses in food products—a review. *Food Research International* **41,** 850–868.

Jamme F, Robert R, Bouchet B, Saulnier L, Dumas P, Guillon F. 2008. Aleurone cell walls of wheat grain: high spatial resolution investigation using synchrotron infrared microspectroscopy. *Applied Spectroscopy* **62,** 895–900.

Jones L, Seymour GB, Knox JP. 1997. Localization of pectic galactan in tomato cell walls using a monoclonal antibody specific to (1→4)-β-D-galactan. *Plant Physiology* **113,** 1405–1412.

Kellogg EA. 2001. Evolutionary history of the grasses. *Plant Physiology* **125,** 1198–1205.

Knox JP. 2008. Revealing the structural and functional diversity of plant cell walls. *Current Opinion in Plant Biology* **11,** 308–313.

Knox JP, Linstead PJ, King J, Cooper C, Roberts K. 1990. Pectin esterification is spatially regulated both within cell walls and between developing tissues of root apices. *Planta* **181,** 512–521.

Larre C, Penninck S, Bouchet B, Lollier V, Denery-Papini S, Guillon F, Rogniaux H. 2010. *Brachypodium distachyon* grain: identification and subcellular localization of storage proteins. *Journal of Experimental Botany* **61,** 1771–1783.

Laudencia-Chingcuanco DL, Vensel WH. 2008. Globulins are the main seed storage proteins in Brachypodium distachyon. *Theorical and Applied Genetics* **117,** 555–563.

Lazaridou A, Biliaderis CG, Izydorczyk MS. 2007. Cereal β-glucans: structure, physical properties, and physiological functions. In: Biliaderis CG, Izydorczyk MS, eds. *Functional food carbohydrates*. Boca Raton, FL: CRC Press, Taylor Francis Group, 1–72.

Lazaridou A, Chornick T, Izydorczyk MS. 2008. Variations in morphology and composition of barley endosperm cell walls. *Journal of the Science of Food and Agriculture* **88,** 2388–2399.

Li L, Shewry P, Ward JL. 2008. Phenolic acids in wheat varieties in the HEALTHGRAIN diversity screen. *Journal of Agricultural and Food Chemistry* **56,** 9732–9739.

Manthey FA, Hareland GA, Huseby DJ. 1999. Soluble and insoluble dietary fiber content and composition in oat. *Cereal Chemistry* **76,** 417–420.

Marcus SE, Verhertbruggen Y, Hervé C, Ordaz-Ortiz JJ, Farkas V, Pedersen HL, Willats WGT, Knox JP. 2008. Pectic homogalacturonan masks abundant sets of xyloglucan epitopes in plant cell walls. *BMC Plant Biology* **8,** 60–72.

Meikle PJ, Hoogenraad NJ, Bonig I, Clarke A, Stone BA. 1994. A (1–3) (1–4)-β-glucan-specific monoclonal-antibody and its use in the quantitation and immunocytochemical location of (1–3) (1–4)-β-D-glucans. *The Plant Journal* **5,** 1–9.

Miller SS, Fulcher RG, Sen A, Arnason JT. 1995. Oat endosperm cell walls: isolation, composition, and comparison with other tisues. *Cereal Chemistry* **75,** 421–427.

Morall P, Briggs DE. 1978. Changes in cell wall polysaccharides of germinating barley grains. *Phytochemistry* **17,** 1495–1502.

Mosse J. 1990. Nitrogen-to-protein conversion factor for ten cereals and six legumes or oilseeds. A reappraisal of its definition and determination. Variation according to species and to seed protein content. *Journal of Agricultural and Food Chemistry* **38,** 18–24.

Opanowicz M, Vain P, Draper J, Parker D, Doonan JH. 2008. *Brachypodium distachyon*: making hay with a wild grass. *Trends in Plant Science* **13,** 172–177.

Ordaz-Ortiz JJ, Devaux M-F, Saulnier L. 2005. Classification of wheat varieties based on structural features of arabinoxylans as revealed by endoxylanase treatment of flour and grain. *Journal of Agricultural and Food Chemistry* **53,** 8349–8356.

Oscarsson M, Andersson R, Salomonsson A-C, Aman P. 1996. Chemical composition of barley samples focusing on dietary components. *Journal of Cereal Science* **24,** 161–170.

Peyron S, Abecassis J., Autran JC, Rouau X. 2001. Enzymatic oxidative treatments of wheat bran layer: effects of ferulic acid composition and mechanical properties. *Journal of Agricultural and Food Chemistry* **49,** 4694–4699.

Philippe S, Saulnier L, Guillon F. 2006. Arabinoxylan and (1→3), (1→4)-β-glucan deposition in cell walls during wheat endosperm development. *Planta* **224,** 1–13.

Philippe S, Tranque O, Utille J-P, Saulnier L, Guillon F. 2007. Ferulic acid in walls of endosperm of mature and developing wheat. *Planta* **225,** 1287–1299.

Robert P, Marquis M, Barron C, Guillon F, Saulnier L. 2005. FT-IR investigation of cell wall polysaccharides from cereal grains. Arabinoxylan infrared assignment. *Journal of Agricultural and Food Chemistry* **53,** 7014–7018.

Saulnier L, Guillon F, Sado P-E, Rouau X. 2007*a*. Plant cell wall polysaccharides in storage organs: xylans (Food applications). In: Voragen AGJ, Kamerling JP, eds. *Comprehensive glycoscience*, Vol. 2. Oxford: Elsevier Science Ltd, 653–689.

Saulnier L, Marot C, Chanliaud E, Thibault J-F. 1995. Cell wall polysaccharide interactions in maize bran. *Carbohydrate Polymers* **26,** 279–287.

Saulnier L, Robert P, Grintchenko M, Jamme F, Bouchet B, Guillon F. 2009. Wheat endosperm cell walls: spatial heterogeneity of polysaccharide structure and composition using micro-scale enzymatic fingerprinting and FT-IR microspectroscopy. *Journal of Cereal Science* **50,** 312–317.

Saulnier L, Sado P-E, Branlard G, Charmet G, Guillon F. 2007*b*. Wheat arabinoxylans: exploiting variation in amount and composition to develop enhanced varieties. *Journal of Cereal Science* **46,** 261–281.

Shibuya N, Iwasaki T. 1978. Polysaccharides and glycoproteins in the rice endosperm cell wall. *Agricultural Biology and Chemistry* **42,** 2259–2266.

Shibuya N, Nakane A. 1984. Pectic polysaccharides of rice endosperm cell walls. *Phytochemistry* **23,** 1425–1429.

Sørensen I, Pettolino FA, Wilson SM, Doblin MS, Johansen B, Bacic A, Willats WG. 2008. Mixed-linkage (1→3) (1→4)-β-D-glucan is not unique to the Poales and is an abundant component of Equistem arvense cell walls. *The Plant Journal* **54,** 510–521.

Tosh SM, Brummer Y, Wood PJ, Wang Q, Weisz J. 2004. Evaluation of structure in the formation of gels by structurally diverse (1→3) (→4)-β-glucans from four cereal and one lichen species. *Carbohydrate Polymers* **57,** 249–259.

Trethewey JAK, Campbell LM, Harris PJ. 2005. (1→3) (1→4)-β-D-Glucans in the cell walls of the Poales (sensu lato): an immunogold labeling using a monoclonal antibody. *American Journal of Botany* **92,** 1669–1683.

Trethewey JAK, Harris PJ. 2002. Location of (1–3)- and (1–3), (1–4)-β-D-glucans in vegetative cell walls of barley (*Hordeum vulgare*) using immunogold labelling. *New Phytologist* **154,** 347–358.

Vain P, Worland B, Thole V, Mckenzie N, Alves SC, Opanowicz M, Fish L, Bevan M, Snape JW. 2008. Agrobacterium-mediated transformation of the temperate grass *Brachypodium distachyon* (genotype Bd 21) for T-DNA insertional mutagenesis. *Plant Biotechnology Journal* **6,** 236–245.

Verhertbruggen Y, Knox JP. 2006. Pectic polysaccharides and expanding cell walls. In: Verbelen JP, Vissenberg K, eds. *The expanding cell. Plant Cell Monographs*, Vol. 5. Berlin: Springer Verlag, 139–158.

Vogel JP, Gu YQ, Twigg P, Lazo GR, Laudencia-Chingcuanco D, Hayden DM, Donze TJ, Vivian LA, Stamova B, Coleman-Derr D. 2006. EST sequencing and phylogenetic analysis of the model grass *Brachypodium distachyon*. *Theoretical and Applied Genetics* **113,** 186–195.

Vogel J, Hill T. 2008. High-efficiency Agrobacterium-mediated transformation of *Brachypodium distachyon* inbred line Bd21-3. *Plant Cell Reports* **27,** 471–478.

Voragen AGJ, Coenen GJ, Verhoef RP, Schol HA. 2009. Pectin: a versatile polysaccharide present in plant cell walls. *Structural Chemistry* **20,** 263–275.

Willats WGT, Marcus SE, Knox JP. 1998. Generation of monoclonal antibody specific to (1–5)-α-L-arabinan. *Carbohydrate Research* **308,** 149–152.

Wilson SM, Burton RA, Doblin MS, Stone BA, Newbigin EJ, Fincher GB, Bacic A. 2006. Temporal and spatial appearance of wall polysaccharides during cellularization of barley (Hordeum vulgare) endosperm. *Planta* **224,** 655–667.